



ISSN: 0975-833X

## RESEARCH ARTICLE

### MODIFICATION IN CHEMICAL, STRUCTURAL AND MORPHOLOGICAL PROPERTIES OF FLY ASH THROUGH MECHANICAL ACTIVATION

<sup>1</sup>Anita Sharma and <sup>2</sup>Ashu Rani

<sup>1</sup>Department of Chemistry, S.S. Jain Subodh P.G. (Autonomous) College, Rambagh Circle, Jaipur, Rajasthan, India

<sup>2</sup>Department of Pure and Applied Chemistry, University of Kota-324005, Rajasthan, India

#### ARTICLE INFO

##### Article History:

Received 19<sup>th</sup> December, 2014  
Received in revised form  
15<sup>th</sup> December, 2014  
Accepted 05<sup>th</sup> January, 2015  
Published online 28<sup>th</sup> February, 2015

##### Key words:

Fly ash, Mechanical activation,  
Acid treatment, Deposition-precipitation,  
Method and ball milling.

Copyright © 2015 Anita Sharma and Ashu Rani. This is an open access article distributed under the Creative Commons Attribution License, which permits unrestricted use, distribution, and reproduction in any medium, provided the original work is properly cited.

#### ABSTRACT

This paper is a critical overview on the experimental results on development of activation techniques to improve the catalytic activity of coal fly ash, in relation to its use as solid acid catalyst and catalytic support materials. Mechanical activation results in slight increase in silica percentage, amorphous nature, specific surface area and surface roughness, as evident by analytical measurements using XRF, XRD, FT-IR, BET surface area, TGA-DTA and SEM techniques. The mechano-chemical activation cangenerate sufficient activity on fly ash surface rendering its potential application in heterogeneous acid catalysis.

## 1.1. INTRODUCTION

Fossil fuel coal which is composed of combustible organic matter with variable amount of inorganic mineral matter is used in modern power station to produce electricity. Several billion metric tons of coal is mined per year throughout the world for use in combustion processes. During combustion of coal, beside energy, a variety of by-products are also produced such as fly ash, bottom ash and flue gas and desulfurization sludge (**The Italian approach to the problem of fly ash, 1999**) Out of all the by-products fly ash is the major solid waste produced after the coal combustion. Fly ash is estimated to be produced up to 600 million tons per year in the world (**Yao et al., 2009**) and about 110 million tons in India (**Senapati, 2011**). Fly ash is used as a supplementary cementitious material (SCM) in the production of portland cement concrete. The mineral parts present in solid fuel coal include clay, micas, quartz, feldspars, sulphides, carbonates of iron, calcium, magnesium etc. During combustion, these minerals become fluid at high temperature and are then cooled. The combustible gasification takes place in furnace of coal fired boiler at an operative temperature 1450°C (2500F) under reducing atmosphere (**Koby, 2008**). At these temperatures the mineral matter within the coal may oxidize, decompose, fuse, disintegrate and fly ash comes from small drops of melt and volatile compounds which are carried up by the ascending

gases. The mixture of gases is cooled where fly ash gets solidify at temperature from 950°C to 400°C. Rapid cooling in the post combustion zone results in the formation of spherical particles known as fly ash consisting of silica, alumina, iron oxide, lime, magnesia and alkali in varying amounts with some unburned activated carbon (**Kutchko and Kim, 2006; Dogen et al., 2006; Fan and Brown, 2001**) and possesses large surface area. Fly ash containing more than 70% SiO<sub>2</sub>, Al<sub>2</sub>O<sub>3</sub> and Fe<sub>2</sub>O<sub>3</sub> and less than about 5% CaO are classified as class F-fly ash and those containing higher CaO are referred to as class C-fly ash (**Kumar et al., 2007**). Higher SiO<sub>2</sub> and Al<sub>2</sub>O<sub>3</sub> of fly ash make it suitable to be used as solid catalyst and catalyst support for heterogeneous catalytic reactions important to industrial sectors. To improve activity of fly ash, several activation techniques such as mechanical, thermal and chemical activation are being used. FA is transformed from micron sized to nano structured through high energy planetary ball milling (**Rao et al., 2010**). Such mechanical activation not only improves degree of fineness but also involves breaking of bonds, dispersion of solids, generation and migration of chemical moieties in the bulk thus results in increased surface roughness and specific surface area (**Kumar et al., 2007**). The modification of morphology and size of FA experienced with milling confreres a great degree of reactivity to the FA as a catalyst or catalyst support material which can be further improved by combining the effects achieved with acid activation (**Blanco et al., 2005**). The detailed results of change in properties of fly ash during mechanical activation are described in this paper.

\*Corresponding author: Ashu Rani,  
Department of Pure and Applied Chemistry, University of Kota-  
324005, Rajasthan, India.

## 1.2. MATERIALS AND METHODS

Fly ash for the present work was collected from Tata Thermal Power Plant (TTPP) situated at Jamshedpur, Jharkhand. The collected F-type fly ash sample has more than 70% of silica and alumina which makes fly ash, a suitable catalytic support material for loading of other chemicals on its surface by various activation techniques.

### 1.2.1 Activation procedure

#### Mechanical activation

The importance of mechanical activation in developing applications of fly ash is to result in bulk utilization with significant value addition. The term 'mechanical activation' refers to enhanced reactivity of fly ash from combined effects of increased surface area and physicochemical changes induced in the bulk as well as on the surface. During the process of mechanical activation, bulk changes e.g. creation of structural defects, structural rearrangements and phase transformation and creation of new surface and surface modification can significantly alter the reactivity of fly ash.

Several techniques, under the broad classification of mechanical activation has been attempted to enhance the silica content and surfacial properties of fly ash. For this purpose the fly ash is mechanically activated using high energy planetary ball mill. Various methods for mechanical activation are as: Prolonged grinding (Arjunan, 2005; Ash Symposium 2005), micro-grinding or milling and sieving. All the three techniques have good effect and have its own advantages and disadvantages. During the present work planetary ball mill is used for mechanical activation.

#### Experimental Procedure

Fly ash was washed with distilled water followed by drying at 100°C for 24h. Dried fly ash was mechanically activated using high energy planetary ball mill (Retsch PM-100, Germany) in an agate grinding jar using agate balls of 5 mm ball sizes for 5, 10 and 15 hours with 250 rpm rotation speed. The ball mill was loaded with ball to powder weight ratio (BPR) of 10:1. Mechanically activated fly ash was calcined at 900°C for 4h for removing carbon, sulphur and other impurities before characterization.

### 1.3 Characterization techniques

Fly ash samples before and after mechanical and thermal activations were analyzed by X-ray fluorescence spectrometer (Philips PW1606). The BET surface area was measured by N<sub>2</sub> adsorption-desorption isotherm study at liquid nitrogen temperature (77 K) using Quantachrome NOVA s1000e surface area analyzer. Powder X-ray diffraction studies were carried out by using (Philips X'pert) analytical diffractometer with monochromatic CuK $\alpha$  radiation ( $k = 1.54056 \text{ \AA}$ ) in a  $2\theta$  range of 0-80°. Crystallite size of the crystalline phase was determined from the peak of maximum intensity ( $2\theta = 26.57^\circ$ ) by using Scherrer formula (Cullity and Stock, 2001) as Eq. (1) with a shape factor (K) of 0.9.

$$\text{Crystallite size} = K \cdot \lambda / W \cdot \cos\theta \quad \dots\dots\dots (1)$$

Where,  $W = W_b - W_s$ ;  $W_b$  is the broadened profile width of experimental sample and  $W_s$  is the standard profile width of reference silicon sample. The FT-IR study of the samples was done using FT-IR spectrophotometer (Tensor-27, Bruker, Germany) in DRS (Diffuse Reflectance Spectroscopy) system by mixing the sample with KBr in 1:20 weight ratio. The Bronsted and Lewis acidity of the catalysts were measured by pyridine adsorbed FT-IR (Tensor-27, Bruker, Germany, with DRS). The detailed imaging information about the morphology and surface texture of the sample was provided by SEM-EDAX (Philips XL30 ESEM TMP).

## 1.4 RESULT AND DISCUSSION

### 1.4.1 Chemical composition

The chemical composition of as received fly ash (FA) and mechanically activated fly ash (MFA) samples milled for 5, 10 and 15h, as analyzed by XRF are given in Table 1.1. Fly ash sample contained high SiO<sub>2</sub>, Al<sub>2</sub>O<sub>3</sub>, Fe<sub>2</sub>O<sub>3</sub> as major percentage and other inorganic oxides are present in low %. Variation in composition of metallic oxides with milling time can be observed in Table 1.1. Which indicates that percentage of alumina reduces marginally and the percentage of silica increases marginally on increasing milling time from 5h to 15h (Paul et al., 2007) and there after it remains unaffected with milling time. TiO<sub>2</sub> percent decreases and those of CaO and Fe<sub>2</sub>O<sub>3</sub> marginally increase with long hours of milling (Rao et al., 2010).

**Table 1.1. Chemical composition of FA and MFA (5h, 10h, and 15h) determined by XRF technique**

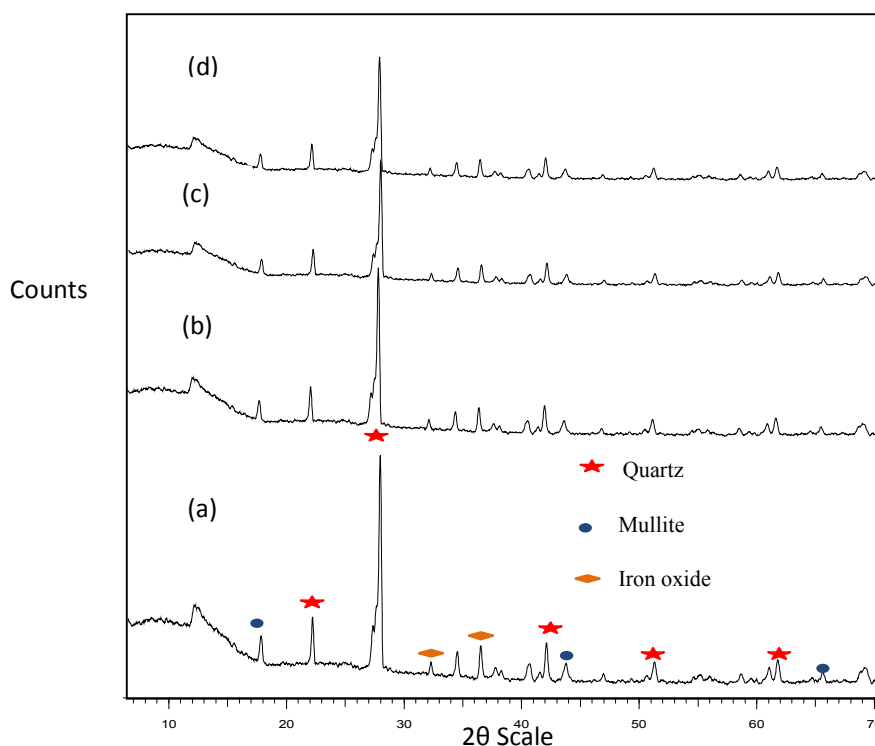
Chemical components	FA	MFA		
		5h	10h	15h
SiO <sub>2</sub>	61.9	62.2	63	66
Al <sub>2</sub> O <sub>3</sub>	29.7	29.6	29.5	28.2
Fe <sub>2</sub> O <sub>3</sub>	2.65	2.65	2.66	2.67
CaO	0.46	0.47	0.47	0.48
MgO	0.36	0.35	0.29	0.24
TiO <sub>2</sub>	1.33	1.32	1.31	1.28
Na <sub>2</sub> O	0.14	0.14	0.13	0.10
K <sub>2</sub> O	0.79	0.79	0.76	0.13
Other elements	2.67	2.48	1.88	0.90
LOI	2.6	2.6	2.0	1.85

### 1.4.2 Structural properties

Structural properties of fly ash samples and change in intensity of crystalline phases of fly ash with mechanical activations are given in Table 1.2 respectively. Table 1.2 presents different mineral phases, their  $2\theta$  value, and intensity count and crystallite size of each phase after 5 to 15h milling time. The broad gibbosity in XRD patterns in the range  $2\theta$  is between 15-35° indicating the coexistence of amorphous components which increases after mechanical activation but decreases after thermal activation of fly ash. As compared with FA, the crystallite size is reduced as milling time was increase up to 15h but the crystallinity and crystallite size of thermally activated fly ash is higher than that of samples before activation due to increases in the crystalline phases.

**Table 1.2. Effect of mechanical activation on intensity of different crystalline phases for FA (XRD detail of MFA)**

Crystalline phases	2 $\theta$	FA		MFA-5h		MFA-10h		MFA-15h	
		Intensity Counts	Crystallite size (nm)						
Mullite	~16	27.2	60	27.2	59	27.1	58	27.0	57
Quartz	~20	37.2	58	37.2	57	37.1	57	37.0	55
Quartz	~26	100	68	100	67	100	66	100	65
Calcite	~30	18.4	54	17.0	54	17.1	52	17.0	51
Hematite	~33	20.5	69	20.6	68	20.6	67	20.5	66
Magnetite	~35	21.0	56	20.4	55	20.3	54	20.2	53
Quartz	~39	18.4	26	18.1	25	18.0	25	17.9	24
Calcite	~40	20.5	50	20.9	49	20.8	48	20.7	47
Mullite	~42	17.8	36	17.5	28	17.4	26	17.3	25
Calcite	~50	17.3	54	16.2	53	16.1	52	16.0	52
Quartz	~54	12.1	33	10.7	29	10.6	27	10.5	25
Quartz	~60	17.9	32	17.8	18	17.6	19	17.5	21

**Figure 1.1. XRD of (a) RFA (b) MFA-5 (c) MFA-10 (d) MFA-15**

The X-Ray diffraction patterns of the fresh as well as ball milled fly ash are given in the Figure 1.1. A steady decrease in the crystallite size is observed and the quartz phase suffers the most. The same effect can be seen in the variation of peak height with milling time (Shaw *et al.*, 2003). The peaks at 16.4°, 42.2° and 26.2° show mullite (alumino silicate) phases while quartz (silica) exhibits strong peaks at 20.7°, 26.5°, 26.66°, 40.66°, 49.96° and 54.2° of 2 $\theta$  values. Peak at 33.56° and 35.62° indicate iron oxide phases (Willians *et al.*, 2005). The 15h ball milling decreases the crystallinity of the fly ash, thus increases the amorphous domains in it. The peak intensity of quartz phase is reduced with increases in the milling hours (5h-15h).

#### 1.4.3 FT-IR studies

The FT-IR spectra of different FA and MFA samples are given in Figure 1.2, show a broad band between 3600-3000  $\text{cm}^{-1}$ , which is attributed to surface -OH groups of Si-OH and

adsorbed water molecules on the surface. The broadness of the band is due to the strong hydrogen bonding. A peak at 1608, 1613 and 1680  $\text{cm}^{-1}$  in the spectra of both inactivated and activated fly ash samples is attributed to bending mode ( $\delta_{\text{O-H}}$ ) of water molecule. Peaks at 1100  $\text{cm}^{-1}$  correspond to Si-O-Si asymmetric stretching vibrations (Patil and Anandhan, 2012). Comparison of the characteristic absorbance range of various chemical functional groups/vibration bands of FA and MFA samples are given in Table 1.3

The increment in broadness between 3600-3300  $\text{cm}^{-1}$  after ball milling at 5 to 15h is an evidence for the breaking down of the quartz structure and formation of Si-OH groups. However, FT-IR studies clearly show changes in the broadening of IR peaks corresponding to Si-O-Si asymmetric stretching vibrations (1161  $\text{cm}^{-1}$ ) indicating structural rearrangement during 15h mechanical milling. Comparison of FT-IR spectra of FA and MFA shown in Figure 1.2 which clearly show changes in the

intensity of IR peaks corresponding to Si-O-Si symmetric stretching ( $697\text{ cm}^{-1}$ ) and T-O-Si (T = Si, Al) asymmetric stretching ( $1161\text{ cm}^{-1}$ ) after milling indicating structural rearrangement during mechanical activation.

different shapes and sizes, hollow, cenospheres, irregularly shaped unburned carbon particles, mineral aggregates and agglomerated particles, whereas the typical SEM images of mechanically activated fly ash samples show

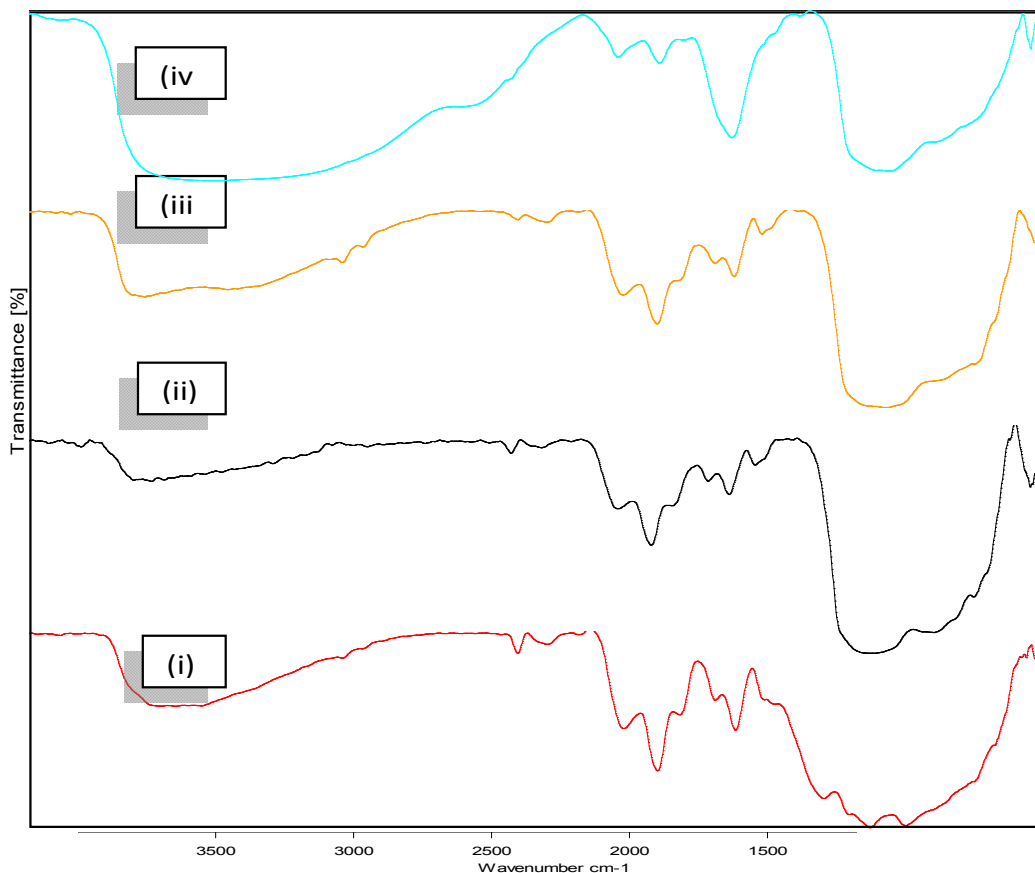


Figure 1. 2. FT-IR spectra of mechanically activated fly ash i) FA, (ii) MFA-5 (iii) MFA-10 and iv) MFA-15

Table 1.3. Result of FT-IR bands for mechanically activated fly ash (MFA)

S. No.	Chemical Functional groups/Vibration band	Characteristics absorption range, Wavelength ( $\text{cm}^{-1}$ )			
		FA (As received fly ash)	MFA (5h)	MFA (10h)	MFA (15h)
1.	Surface-OH group of $\text{SiOH}/\text{Al}_2\text{O}_3$ (Maxima.)	3632	3432	3446	3583
2.	O-H Stretch (Alcoholic & water)	3553	3301	3303	3305
3.	C-H stretching vibration	2827	-	-	-
4.	$\nu$ OH stretching	2343	-	2338	2342
5.	H-SiO <sub>3</sub>	2241	-	-	-
6.	=Si-H (monohydride)	1984	1989	1989	1988
7.	Calcium Carbonate	1872	1870	1870	1870
8.	H-O-H bending vibration	1681	1614	1614	1613
9.	CaO	1524	1524	1525	1524
10.	Si-O-Si asymmetric stretching	1100	1095	1094	1090
11.	Si-O-Ca stretching	-	1050	1050	1046
12.	Carbonate group	-	-	-	697
13.	Calcium oxide (CaO)	610	610	611	610
14.	C-OH, TWIST	570	565	564	562

MFA-5 (5 hr milled fly ash); MFA-10 (10 hr milled fly ash); MFA-15 (15hr milled fly ash)

### 1.4.4 SEM analysis

The SEM images of FA and MFA samples are shown in Figure 1.3 to 1.4. The investigation reveals that most of the particles present in the FA samples are spherical in shape with relatively smooth surface consisting of quartz, clusters of iron particles formed due to partial decomposition of pyrite and dark quartz inclusions (Offler, 1996). Fly ash demonstrates particles of

the structural changes of larger particles and increased surface roughness which is increased with increase in milling time 5 to 15h (Figure 1.4).

The smooth spherical cenospheres are affected most resulting remarkable changes in morphology and breaking of spherical silica structure.

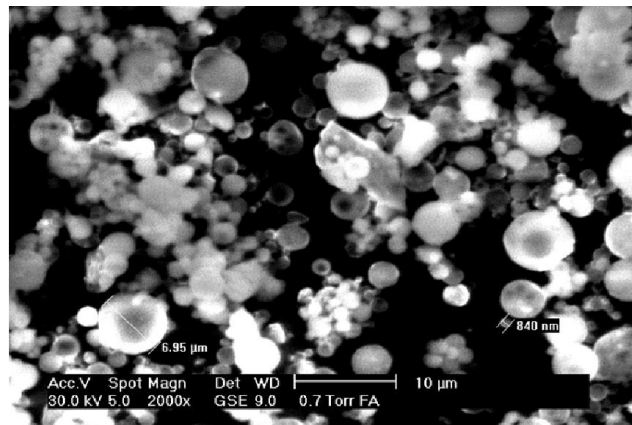


Figure 1.3. SEM micrograph of pure fly ash (FA)

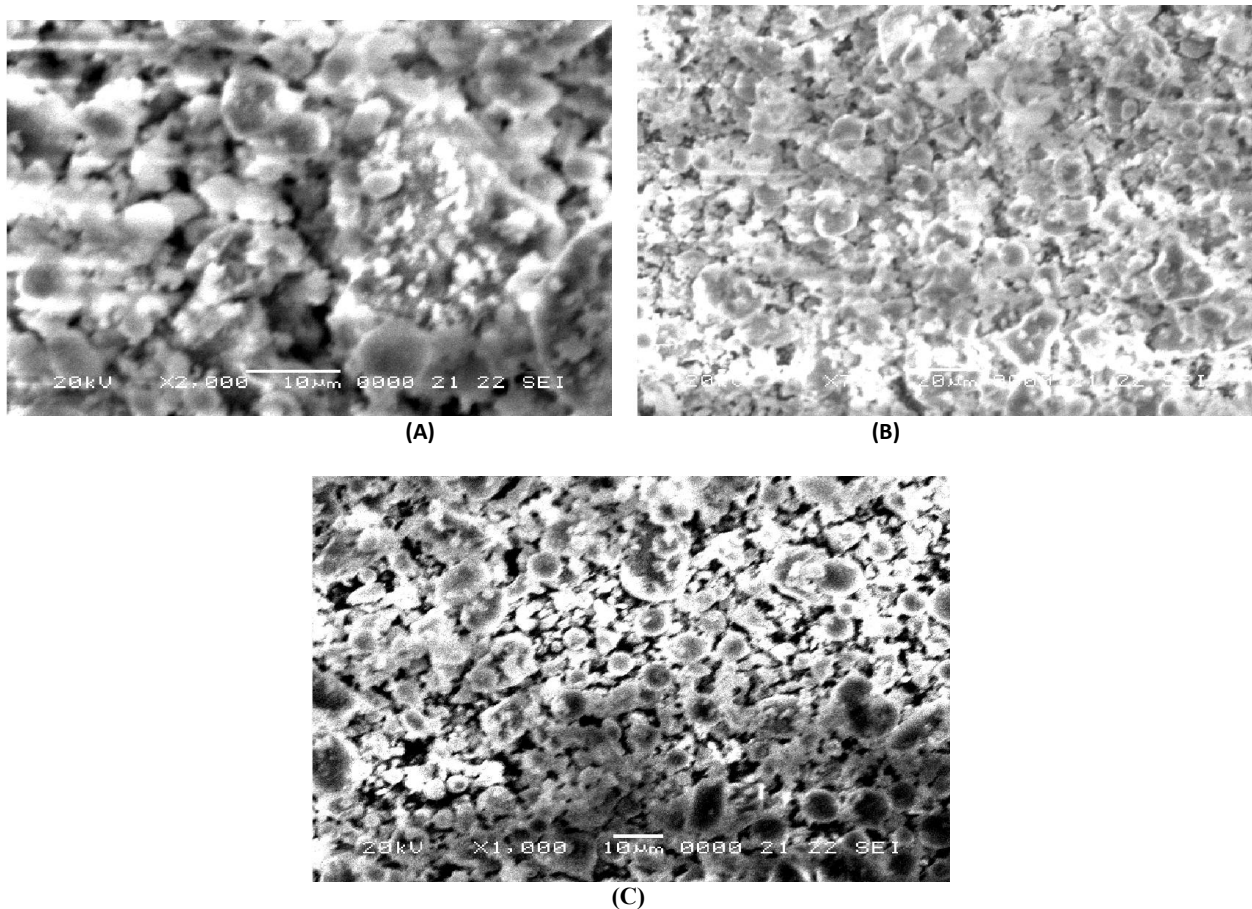


Figure 1.4 SEM micrographs of (A) MFA-5h, (B) MFA-10h and (C) MFA-15h

#### 1.4.5 BET Surface area

The mechanical activation of fly ash affects its surface properties. The variation in BET surface area of FA with different milling time and temperature is shown in Table 1.4 which indicates that the BET surface area is increased marginally after milling for 5 to 15h and increased from 0.97 m<sup>2</sup>/g to 2.57 m<sup>2</sup>/g, (Willians *et al.*, 2005).

This result confirms that the mechanically activated (15h) fly ash has a higher specific surface area of 2.57 m<sup>2</sup>/g than the fly ash with 0.97 m<sup>2</sup>/g (Rao *et al.*, 2010; Legodi *et al.*, 2001).

Table 1.4. Characterization of fly ash before and after activation

Samples	FA	MFA		
		MFA 5h	MFA 10h	MFA 15h
BET surface area (m <sup>2</sup> /g)	0.97	1.88	2.46	2.57

#### 1.4.6 TGA-DTA analysis

Figure 1.5 shows the TG-DTA curves of the coal fly ash. The DTA curve shows three exothermic peaks at 580°C, 700°C and 950°C during the heating process, while no exothermic peak is observed during the cooling process. Thus, the exothermic

peaks are attributable to an irreversible reaction. The TG curve began to decrease at 580°C and reached a steady state at over 950°C (Hasezaki *et al.*, 2007; Versan Kok, 2002). It is speculated that the exothermic peak at 580°C in air was due to combustion of the unburned carbon in the coal fly ash, which led to a mass decrease. The exothermic peaks at 700 and 950°C could have resulted from evaporation of Na<sub>2</sub>O and K<sub>2</sub>O alkali oxides of low melting point and crystallization of the glass phase

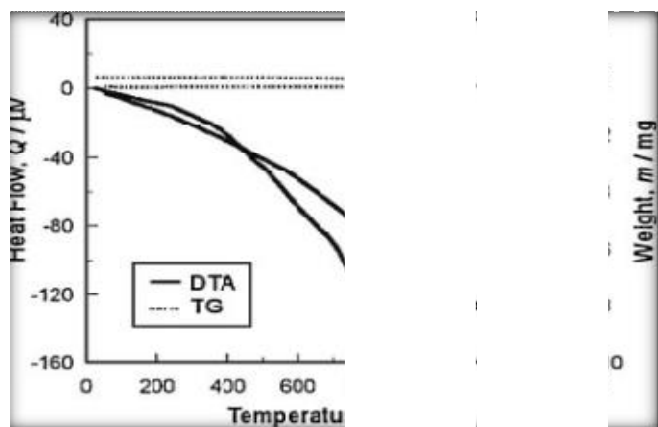


Figure 1.5. TGA-DTA curves of fly ash

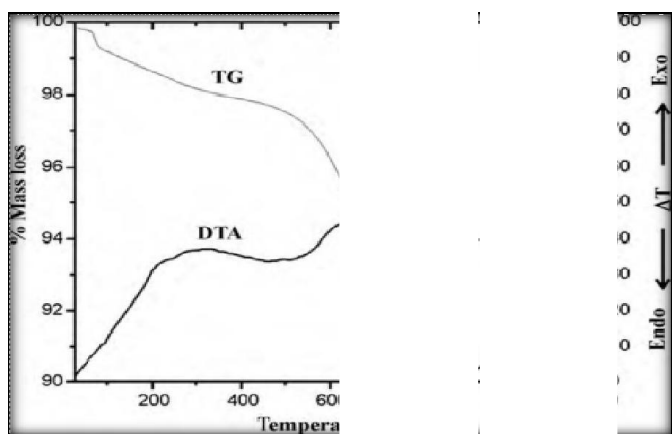


Figure 1.6. Differential and gravimetric thermal analysis of MFA

TGA and DTA analysis curves of MFA (15h milling) are shown in Figure 1.6 which indicates that there are three important changes (i) the first is a loss of weight between room temperature and 100°C related to the loss of humidity, (ii) then from 100 to 450°C, hydration water is lost, (iii) between 450°C and 700°C, there is a further loss of weight attributed mainly to the decomposition of CaCO<sub>3</sub> and the burning of residual coal present in the fly ash. Differential thermal analysis shows an additional change above 900°C (Stefanovi *et al.*, 2007; Nie *et al.*, 1993; Liu *et al.*, 1993).

It is interesting to get different TGA and DTA curves for mechanically activated fly ash from raw fly ash, which also confirms that there are same morphological changes in mineral phases during milling.

## 1.5 Conclusion

FA contains high silica content, which helps in converting it as an active catalytic material like other silica sources. After suitable activation and modified surface activity, FA can be converted as an active catalytic support for synthesis of heterogeneous catalyst for various organic transformations. The mechanical activation of fly ash using high energy ball mill affects the surface properties of the fly ash more than the other properties. FA can be transformed from micron sized to nano structured through high energy planetary ball milling. Such mechanical activation not only improves degree of fineness but also involves breaking of bonds, dispersion of solids, generation and migration of chemical moieties in the bulk thus results in increased surface roughness and specific surface area. Transformation of quartz and cristobalite phases into a glassy phase is also faster in MFA. With increase in milling duration from 5h to 15h silica percentage is marginally changed whereas the crystallite size of crystalline phase is reduced and specific surface area is increased from 1.88 to 2.57 m<sup>2</sup>/g. It is concluded that the modification properties of FA can be achieved by mechanical activation methods to generate degree of reactivity on FA in the form of surface silanol groups as a catalyst or catalyst support material.

## 1.6 REFERENCES

- Arjunan, P. *Fly ash India*, 2005.
- Ash Symposium 2005. International conference 'World of coal Ash 2005, 20-25 (<http://whocares.caer.uky.edu/wasp/AshSymposium>).
- Blanco, F., Garcia, M. P. and Ayala, J. 2005. Variation in fly ash properties with milling and acid leaching. *Fuel*, 84, 89-96.
- Cullity, B. D. and Stock, S. R. 2001. *Upper Saddle River. NJ: prentice Hall; third ed.* 388.
- Dogen, O. and Kobya, M. J. 2006. *Quant. Spectro. Rediat. Trans.* 101, 146-150.
- Fan, M. R. and Brown, C. 2001. *Energy Fuels*, 15, 1414-1417.
- Hasezaki, K., Nakashita, A., Kaneko, G. and Kakuda, H. 2007. *Mater. Trans.* 48 (12) 3062- 3065.
- Kobya, M. 2008. *Solid Fuel Chem.* 42, 107-119.
- Kumar, R., Kumar, S. and Mehrotra, S. P. 2007. *Resour. Conserv. Recyc.* 52, 157-179.
- Kumar, R., Kumar, S. and Mehrotra, S. P. 2007. Towards sustainable solution for Fly ash through mechanical activation. *Resour. Conserve. Recyc.* 52, 157-179.
- Kutchko, B. G., Kim, A. G. *Fuel* 85 (2006) 2537-2544.
- Legodi, M. A., de Waal, D. J., Potgieter, H. and Potgieter, S. S. 2001. *Miner. Eng.* 14, 1107-1111.
- Liu, K., Jakob, E., McChMen, W. H. and Meuzelaar, H. L. C. 1993. *ACS Fuel Chem. Div. Preprints* 38 (3) 823-842.
- Nie, X., McClennen, W. H., Liu, K. and Meuzelaar, H. L. C. 1993. *ACS Fuel Chem. Div. Preprints* 38 (4) 1147-1159.
- Offler, L., Lohse, E., Peuker, U., Oehlmann, C. L., Kustov, M. and ZholObenko, V. L. 1996. *Clays and Clay Miner.* 44, 635.
- Patil, G. A. and Anandhan, S. 2012. *Int. J. Energy Eng.* 2, 57-62.
- Paul, K. T., Satpathy, S. K., Manna, I., Chakraborty, K. K. and Nando, G. B. 2007. *Nanoscale Res. Lett.* 2, 397-404.

- Rao, J., Narayanaswami, P. and Prasad, S. 2010. *Int. J. Eng. Sci. Technol.* 2 (5) 284-299.
- Rao, J., Narayanaswami, P. and Shiv Prasad, 2010. Thermal stability of nano structured fly ash synthesized by high energy ball milling. *International J. Eng. Sci. Tech.*, 2(5) 284-299.
- Senapati, M. R. 2011. *Curr. Sci.* 100 (12).
- Shaw, L. L., Ren, R., Ban, Z. and Yang, Z. 2003. *Ame. Ceram. Soc.*, 137, 50-69.
- Stefanovi, G., Ojba, L., Sekuli, I. and Matija, S. 2007. *J. Serb. Chem. Soc.*, 72 (6), 591-604.
- The Italian approach to the problem of fly ash, 1999. *International Ash utilization symposium. Center for applied Energy Research University of Kentucky paper 84.*
- Versan Kok, M. 2002. *Energy Sources* 24 (10), 899-905
- Willians, P. J., Biernacki, J. J., Rawn, C. J., Walker, L. and Bai J. *ACI Mater. J.*, 102 (5) (2005) 330.
- Yao, Z. T., Xia, M. S., Ye, Y. and Hazard, J. 2009. *Mater* 170 (2), 639-644.

\*\*\*\*\*